SMAR 2019 – Fifth Conference on Smart Monitoring,
Assessment and Rehabilitation of Civil Structures

SMAR 2019

Seismic screening approaches for detection of structural changes

Chun-Man LIAO [1], Yuri PETRYNA [1]
[1] Technische Universität Berlin, Berlin, Germany

Contact e-mail: chunman@win.tu-berlin.de

ABSTRACT: The present contribution is dealing with seismic screening of buildings by use of seismic interferometry and wave deconvolution analysis. At that, the artificial wave propagation between two sensor positions is reconstructed from the ambient vibration measurements. The wave propagation velocity within a sensor network can be used to estimate structural stiffness, locally and globally, i.e. depending on the sensor position. The change of the wave characteristics are assumed to be caused by the stiffness change due to damage. This approach is studied on a 14-story building in Bishkek, Kyrgyzstan and a foot bridge in Berlin, Germany. It is compared to a classical operational and numerical modal analysis. Alternatively, the application of the so-called transmissibility functions for damage detection is explained and illustrated. The transmissibility functions can be determined from the ambient vibration measurements of the same kind as used for the wave propagation analysis. A comparison of the both mentioned approaches to seismic screening is currently in progress.

1 INSTRUCTION

Structural Health Monitoring (SHM) is usually related to dynamic properties of the structure like natural frequencies and mode shapes or some other state indicators which can be derived from the global or local vibration response. Even the damage localization can be carried out if the sensor network is dense enough. On the other hand, the non-destructive testing (NDT) frequently uses the wave propagation phenomena to determine local structural properties of the specimen under consideration or their changes due to damage. However, NDT requires a special excitation and is limited to quite local areas.

The wave propagation is also used in the geophysics to determine the soil properties, thus making its layered structure visible. It can be considered as a kind of seismic screening. At that, the ambient vibration measurements on the surface or along the depth of the soil are usually applied. That kind of geophysical analysis has also been applied to buildings by considering them like a layered continuum, see Safak (1999), Todorovska & Trifunac (2008). This is a kind of seismic screening for structures. However, the length of the seismic waves in the structure is more or less comparable with the building height and, therefore, the seismic wave characteristics are less sensitive to local damage.

The proposed approach uses the wave reconstruction from the ambient vibration measurements as well. However, it does not assume the same structural stiffness within each story but takes local stiffness properties into account. It has been shown, for instance, that the wave velocity over the height of the building depends on the sensor position in the story, i.e. the wave propagation is not homogeneous for the whole story. The wave phenomena in the building are more complex than in the layered continuum. By analyzing the wave characteristics between

various sensor positions, it becomes possible to roughly localize the damage. Some limitations of this approach are also shown.

An alternative approach based on the ambient vibration measurements is also applied and checked. It uses the so-called transmissibility functions, see Yan et al. (2019). The latter can be considered as a ratio of frequency response function (FRF) determined at two different measurement positions. This approach seems to be more sensitive to structural changes than the global shear wave propagation in the building. Some open problems of the application of the both approaches, wave reconstruction and transmissibility functions, are subject of ongoing research. Besides, a damage indicator based on the transmissibility function is developed and checked on the example of a footbridge in Berlin. Since do damage is allowed to introduce to the structure, an additional mass is used for this purpose.

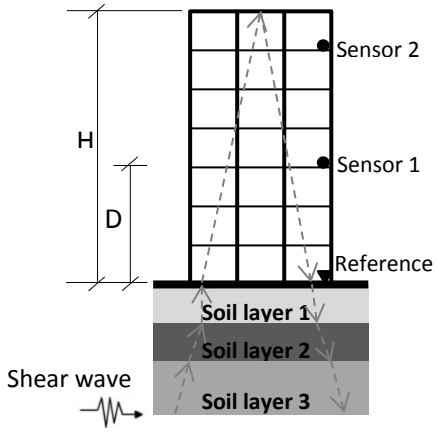

Figure 1. Wave propagation in a building structure.

2 SEISMIC INTERFEROMETRY APPROACH

2.1 Background theory

In this section, the wave propagation analysis employed in the field of soil mechanics is introduced. The ground motion is evoked by a vibration source which is indicated as a shear wave shown in the Fig. 1. We expect the seismic interferometry phenomena happens in the building, whose vibration response inherits the dynamic pattern of the soil. Therefore, the structure above the ground surface is considered as an extending soil layer outside the earth as shown in the Fig.1. The sensor receives the vibration of the entire building structure involving the interaction between the soil and the building. Thus, the dynamic response $V(t)$ recorded at the sensors can be interpreted as the convolution of the transfer function $h(t)$ and the ground motion $P(t)$:

$$V(t) = h(t) \cdot P(t), \tag{1}$$

where $h(t)$ is the transfer function related to the system properties as known for the compliance of the structure or the soil impedance. Additionally, the transfer function $h(t)$ depends on the system, which is constrained by the reference positon and the sensor position.

2.2 *Deconvolution method*

For a linear system, the convolution can be rewritten in frequency domain by the Fourier transform and save the computation. That is,

$$\hat{V}(\omega_i) = \hat{h}(\omega_i) \cdot \hat{P}(\omega_i), \quad i = 0, \dots, N-1 \tag{2}$$

where $\hat{\mathrm{V}}(\omega_\mathrm{i}), \hat{\mathrm{h}}(\omega_\mathrm{i}), \hat{\mathrm{P}}(\omega_\mathrm{i})$ are the Fourier coefficients in frequency domain corresponding to the system response $V(t)$, transfer function $h(t)$ and the vibrational source $P(t)$. N denotes the number of samples in the record.

The Fourier coefficient of the transfer function can be obtained straightforwardly by the deconvolution operation, the division of two signals.

$$\hat{h}(\omega_i) = \frac{\hat{V}(\omega_i)}{\hat{P}(\omega_i)}, i = 0, \dots, N-1. \tag{3}$$

In fact, these two arbitrary signals can be recognized as an output response and an impulse as an input model. The essence of transfer function doesn't change in the deconvolution relation.

For instance, if we have two output measurements $\widehat{V_1}(\omega_i)$ and $\widehat{V_2}(\omega_i)$ at the different levels in the building, the signal $\widehat{V_2}(\omega_i)$ is received at the reference position; and the signal $\widehat{V_1}(\omega_i)$ at the other level in the building is the cut-off system response to the signal $\widehat{V_2}(\omega_i)$. The transfer function between the reference position and the cut-off location is

$$\hat{h}(\omega_i) = \frac{\widehat{V_1}(\omega_i)}{\widehat{V_2}(\omega_i)}, i = 0, \dots, N-1. \tag{4}$$

Following the Eq.(4), the new output response $\hat{\mathrm{G}}(\omega_\mathrm{i})$ at the cut-off location can be predicted by the unchanged transfer function and the known new input model $\hat{\mathrm{F}}(\omega_\mathrm{i})$ at the reference position. That is,

$$\hat{G}(\omega) = \hat{F}(\omega)\hat{h}(\omega). \tag{5}$$

Since

$$\frac{\widehat{V_1}(\omega_i)}{\widehat{V_2}(\omega_i)} \equiv \frac{\hat{G}(\omega_i)}{\hat{F}(\omega_i)}. \tag{6}$$

2.3 *Normalized Input Output Minimization (NIOM) method*

Referencing to Kawakami et al. (1998, 2004), the simplified input and output model in the deconvolution formula is introduced. Base on the Eq.(4), the input at t=0 is normalized to unity by use of $\hat{h}(\omega_i)$ applying the method of Lagrange multipliers. The power spectrum of the new input signal $\mathrm{X}(\omega_i)$ is minimized as shown in Eq. (7). Meanwhile, the new output model $\mathrm{Y}(\omega_i)$ shown in Eq.(8) can be predicted by use of the unchanged transfer function according to the Eq.(5) .

$$\hat{X}(\omega_i) = N\Delta t \frac{\frac{1}{(1+\frac{k_0}{c_0}{\omega_i}^2)+(c_0+c_1|\hat{h}(\omega_i)|^2)}}{\sum_{n=0}^{N-1}\frac{1}{(1+\frac{k_0}{c_0}{\omega_i}^2)+(c_0+c_1|\hat{h}(\omega_i)|^2)}} \tag{7}$$

$$\hat{Y}(\omega_i) = N\Delta t \frac{\frac{\hat{h}(\omega_i)}{(1+\frac{k_0}{c_0}{\omega_i}^2)+(c_0+c_1|\hat{h}(\omega_i)|^2)}}{\sum_{n=0}^{N-1}\frac{1}{(1+\frac{k_0}{c_0}{\omega_i}^2)+(c_0+c_1|\hat{h}(\omega_i)|^2)}} \tag{8}$$

3 TRANSMISSIBILITY FUNCTIONS

A transmissibility function is an expression of a ratio of two responses between two DOFs in frequency domain. Only the output data is considered, that is

$$TF(\omega) = \frac{X_1(\omega)}{X_2(\omega)} \tag{9}$$

On the other hand, the transmissibility function can be constructed by a ratio of frequency response function (FRF) models. As a multi-degree of freedom linear system is considered, the vibration model can be constructed as follows.

$$\begin{Bmatrix} X_1(\omega) \\ X_2(\omega) \\ \vdots \\ X_i(\omega) \end{Bmatrix} = [-\omega^2 \boldsymbol{M} + i\omega \boldsymbol{C} + \boldsymbol{K}]^{-1} \begin{Bmatrix} F_1(\omega) \\ F_2(\omega) \\ \vdots \\ F_j(\omega) \end{Bmatrix} = \boldsymbol{H}_{ij}(\omega) \begin{Bmatrix} F_1(\omega) \\ F_2(\omega) \\ \vdots \\ F_j(\omega) \end{Bmatrix} \tag{10}$$

where $[-\omega^2 \boldsymbol{M} + i\omega \boldsymbol{C} + \boldsymbol{K}]^{-1}$, the inverse of the impedance matrix is the expression of $\boldsymbol{H}_{ij}(\omega)$ and analog to transfer function described in the last section. $\boldsymbol{H}_{ij}(\omega)$ is called FRF matrix.

3.1 Global transmissibility function

According to Eq.(10) and Eq.(9), the ratio of two responses at l-DOF and k-DOF can be presented by use of the FRF matrix:

$$TF_{lk}(\omega) = \frac{X_l(\omega)}{X_k(\omega)} = \frac{\sum_{n=1}^{j} H_{ln}(\omega) F_n(\omega)}{\sum_{n=1}^{j} H_{kn}(\omega) F_n(\omega)} \tag{11}$$

3.2 Local transmissibility function

When there is only one force component for the excitation, we take $F_2(\omega)$ for example. Eq.(11) can be rewritten as the ratio of two entries in the FRF matrix :

$$TF_{lk}(\omega) = \frac{X_l(\omega)}{X_k(\omega)} = \frac{H_{l2}(\omega)}{H_{k2}(\omega)} \tag{12}$$

which equals to a scalar and is called local transmissibility function.

3.3 Damage indicator(DI)

To identify the change of the system after damage exists, the difference between the transmissibility function is contributed to the formulation of DI.

$$DI = \int_{\omega_1}^{\omega_2} \left| TF_{lk}^{undamaged} - TF_{lk}^{damaged} \right| d\omega \tag{13}$$

The higher value of DI points out the severe damage level compared with the undamaged state. This value assists to localize the damage position between any two locations.

4 APPLICATIONS

To verify the applicability of the proposed approach, following examples demonstrated the wave propagation analysis applied to the undamaged building structure and the damage indicator based on the transmissibility function of a footbridge, respectively.

4.1 14-story RC building in Bishkek

The target building is a 14-story reinforced concrete frame structure with a stiff shaft for the stairwell. It is a twofold symmetric structure, except the stairwell. Horizontal stiffening and infill walls are constructed by concrete diaphragms in each story. Figure 2, left shows 3 geophone sensors (at position A, B, C) installed in each floor from story 2 to 13. Position A is close by the stiff core, while position B and position C are adjacent to the outer columns. The sampling rate of the sensors for the ambient vibration measurements was set to 400 Hz.

The building with a total height of 47 m over ground contains a basement. The cross-sections of the columns and the shear walls of the bottom part (basement, stories 1-3) and the upper part of the building (stories 4-13) are different (Fig. 2, right).

Figure 2. Sensor configuration at positions A,B,C (left) and building appearance (right).

The similar modes are extracted in both experimental and numerical way. Operational modal analysis was applied using the ARTEMIS software (Fig. 3, left) and numerical modal analysis by use of the finite element model was performed by software LIRA 9.2 (Fig. 3, right). Figure 3. shows that the first two modes are almost identical and correspond to bending in x- and y-direction. The third mode describes the torsional vibration of the building. The difference between the first two bending modes is caused by a non-symmetric position of the stiff core.

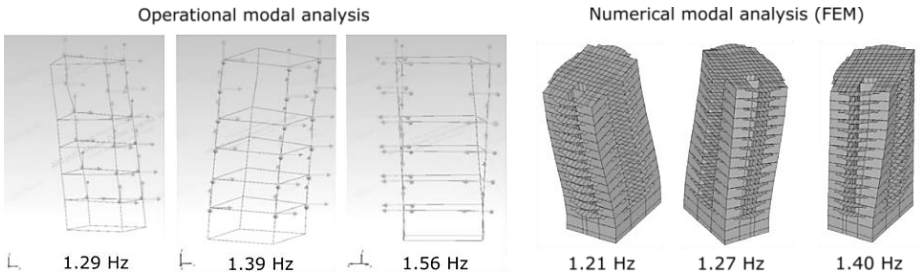

Figure 3. First 3 vibration modes of the building obtained from OMA (left) and FEM (right).

On the other hand, NIOM method was carried out on the frequency spectrum of the ambient vibration measurements (Fig. 4, left). The simplified new input model turned out to be the impulse at 2F (Fig. 4, right).

The output models are regarded as the convolution results of the impulse and the individual transfer function at each floor. By tracing the wave peaks shown with the known floor height, the wave velocity can be predicted by the wave traveling time.

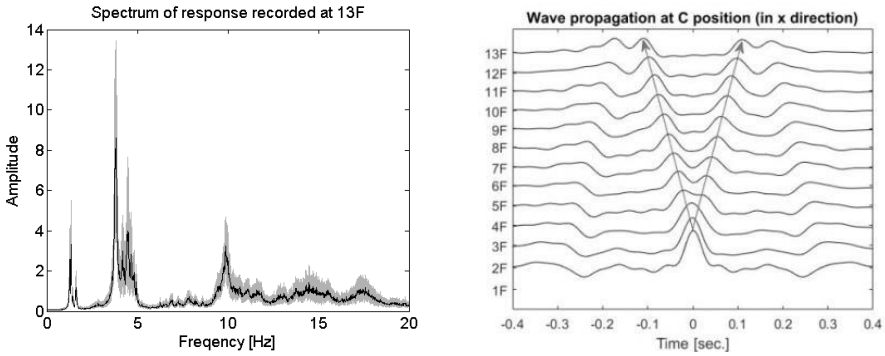

Figure 4. Mean velocity spectral amplitude (left) and deconvolved wave propagation (right).

Table. 1 implies that the wave velocity is sensitive to the structural stiffness, since the vibration recorded closed to stiff stairwell core (position A) reveals the faster wave propagation. Also, the records at the 3 lower floors results in the higher wave velocity than at the upper floors due to the higher stiffness at the building base. The natural frequency obtained by applying the frequency domain decomposition method to the measurements is compared with the wave velocity in Table. 2. Obviously, the wave velocity at positions A,B and C are different, while the natural frequencies remains the same. Is shows a higher sensitivity of the wave propagation to local stiffness changes compared to the integral characteristics like natural vibration frequency.

Table 1. Wave velocity predicted by use of NIOM in x-direction (unit: m/s)

Reference floor	Current floor	Position A	Position B	Position C
2	6	391.1	352.0	364.1
2	8	386.3	360.0	360.0
2	10	377.1	352.0	346.2
2	12	371.8	342.9	334.2

Table 2. Natural frequency and wave velocity in x- and y- direction

	Wave velocity (m/s)		Natural frequency (Hz)	
Direction	*x*	*y*	*x*	*y*
Position A	371.8	400.0	1.29	1.39
Position B	342.9	394.0	1.29	1.39
Position C	334.2	400.0	1.29	1.39

4.2 Foot bridge

A 64m cable-stayed foot bridge in Berlin was investigated by the ambient vibration test with 10 3D geophones, whose configuration is illustrated in the Fig. 5. The sampling rate of the sensors was set to 400 Hz. The main structure consists of two longitudinal steel girders with hollow box cross-sections and lateral T-beams for transverse connection. Six cables are joined to the top of the A-pylon.

Since it is forbidden to introduce a real damage to the bridge, we used an additional mass to change the system properties. The natural frequency of 2.15 Hz determined from the ambient measurements by the FDD method without additional mass changes to 2.15 Hz, 2.02 Hz and 2.00 Hz in the bridge with additional mass on Position 2,7 and 8.

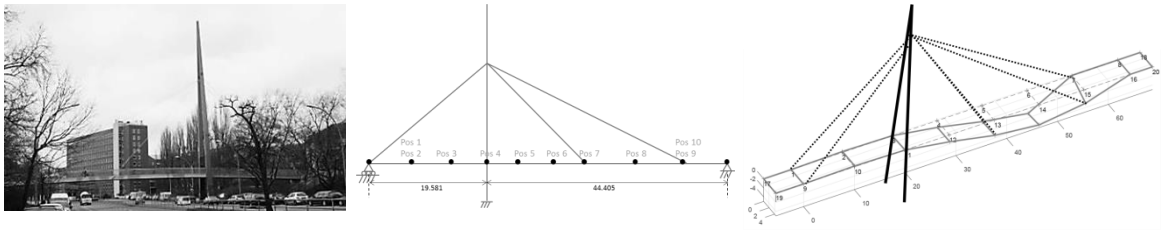

Figure 5. Foot bridge in Berlin (left), sensor configuration (middle) and the 1st mode at 2.15 Hz (right).

The damage indicator calculated from the transmissibility functions according to (13) for various pairs of sensors is shown in Fig. 6. Herein, $DI_{9,8}$ means, for example, the damage indicator value for the transmissibility between positon 9 and 8. Generally, the higher damage indicators correspond to the area where the system property has been changed, except for the position 2.

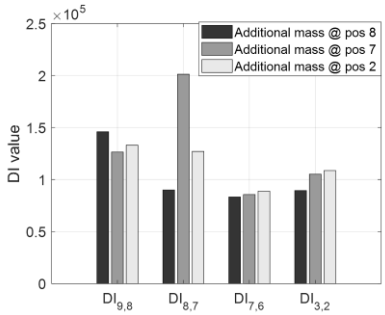

Figure 6. Damage indicator for various sections of the bridge between two sensor locations.

5 CONCLUSIONS

Two methods of seismic screening have been applied to structural assessment in the present study, the seismic interferometry and the transmissibility functions. Both are based on the vibration propagation between sensor positions. It has been shown that the wave propagation is more sensitive to local structural changes than traditional methods based on operational or experimental modal analysis.

Damage indicator based on the transmissibility functions can generally detect and localize the real structural change, as shown for the footbridge. However, the application of seismic

screening approaches is facing with several challenges that are subject of the ongoing research. Some of them will be illustrated and discussed during the conference.

6 ACKNOWLEDGEMENT

The authors gratefully appreciate financial support of the German Academic Exchange Service (DAAD) and the Government Scholarship to Study Abroad (GSSA) of Taiwan for the first author in the framework of the PhD Research Grants.

7 REFERENCES

Haddadi, H. R., Kawakami, H. 1998. Modeling wave propagation by using normalized input–output minimization (NIOM) mrthod for multiple linear systems. *Struct. Eng./Earthquake Eng*., *JSCE*, 15(1): 29-39.

Kawakami, H., Oyunchimeg, M. 2004. Wave propagation modeling analysis of earthquake records for buildings. *J. Asian Arch. and Building Eng*, 3(1): 33-40.

Rahmani, M., Todorovska, M. 2013. System identification of buildings by wave travel time analysis and layered shear beam models—Spatial resolution and accuracy. *Struct. Control Health Monit*, 20: 686-702.

Safak, E. 1999. Wave–propagation formulation of seismic response of multistory buildings. *J. Struct. Eng*., 125(4): 426-437.

Todorovska, M., Trifunac, M.D. 2008. Impulse response analysis of the Van Nuys 7-storey hotel during 11 earthqaules and earthquake damage detection. *Struct. Control Health Monit*., 15: 90-116.

Todorovska, M. I., Trifunac, M.D. 2008. Earthquake damage detection in the Imperial County Services Building III: Analysis of wave travel times via impulse response functions. *Soil Dynamics and Earthquake Engineering*, 28, 387-404.

Yan, W., Zhao, M., Sun, Q., Ren, W. 2019. Transmissibility-base system identification for structural health monitoring: fundamentals, approaches, and applications. *Mechanical System and Signal Processing*. 117: 453-482.